의학박사 학위논문

인간 피부 이종이식 모델에서 지방유래 줄기세포가 면역 조절 및 이식편 생존에 미치는 영향에 관한 연구

Effect of Adipose-Derived Stem Cells on Immune Modulation and Graft Survival in Human Skin Xenotransplantation Models

2023년 8월

서울대학교 대학원

의학과 성형외과학 전공

전 성 미

A thesis for the degree of Doctor of Philosophy

Effect of Adipose-Derived Stem Cells on Immune Modulation and Graft Survival in Human Skin Xenotransplantation Models

인간 피부 이종이식 모델에서 지방유래 줄기세포가 면역 조절 및 이식편 생존에 미치는 영향에 관한 연구

August 2023

Graduate School
Seoul National University
Plastic and Reconstructive Surgery Major

Sungmi Jeon

인간 피부 이종이식 모델에서 지방유래 줄기세포가 면역 조절 및 이식편 생존에 미치는 영향에 관한 연구

지도교수 김 상 화

이 논문을 의학박사 학위논문으로 제출함

2023년 4월

서울대학교 대학원

의학과 성형외과학 전공

전 성 미

전성미의 의학박사 학위논문을 인준함

2023년 7월

위 원 장 _____ 장 학 _____ (印)

부위원장 _____ 김 상 화 _____ (印)

위 원 _____ 문 제 호 _____ (印)

위 원 _____ 안 상 현 _____ (印)

위 원 _____ 김 연 환 _____ (印)

Effect of Adipose-Derived Stem Cells on Immune Modulation and Graft Survival in Human Skin Xenotransplantation Models

by

Sungmi Jeon

A thesis submitted to the Department of Medicine
at Seoul National University College of Medicine
in partial fulfillment of the requirements for the degree of
Doctor of Philosophy in Plastic and Reconstructive Surgery

April 2023

Approved, Thesis Committee

July 2023

Prof. Hak Chang Chair

Prof. Sang Wha Kim Vice chair

Prof. Je-Ho Mun Member

Prof. Sanghyun Ahn Member

Prof. Youn Hwan Kim Member

Abstract

Background: Adipose-derived stem cells (ADSCs) exert immunomodulatory effects in the treatment of transplant rejection. This study aimed to evaluate the effects of ADSCs on the survival of human skin xenograft onto rodents and to investigate the mechanisms underlying the immunomodulatory effect of ADSCs.

Methods: To evaluate the effect of ADSCs on graft survival and compare the administration methods (intravenous versus subcutaneous injection), C57BL/6 mice were used as recipients of full-thickness human skin xenotransplantation. To compare single versus triple injections of ADSCs and analyze the mechanism of immune response, 2 x 2 cm^2-sized human skin xenografts were transplanted onto the backs of Sprague-Dawley rats. The host rodents were administrated with autologous ADSCs suspended in phosphate-buffered saline (PBS). The rats were euthanized 7, 10, and 14 days after transplantation to assess the mechanism underlying the immunomodulatory effects of ADSCs on human skin xenografts.

Results: Subcutaneous injection of ADSCs appeared to be superior to intravenous injection in a human-to-mouse skin xenotransplantation model. Triple injections of ADSCs considerably delayed cell-mediated xenograft rejection compared with the control (PBS) and single-injection groups in a human-to-rat skin xenograft model. The vascularization and collagen type 1 to 3 ratios in the ADSC group were significantly higher than those in the control group. In addition, intragraft infiltration of CD3-, CD4-, CD8-, and CD68-positive cells was reduced. Furthermore, the expression levels of proinflammatory cytokine interferon-gamma (IFN-γ) were decreased and immunosuppressive prostaglandin E synthase (PGES) was increased in the xenograft and lymph node samples.

Conclusion: This study presented that triple subcutaneous injections of ADSCs was effective improving skin xenograft survival by suppressing cell-mediated xenograft rejection compared with the control and single-injection groups. The immunomodulatory effects of ADSCs were associated with the downregulation of IFN-γ and upregulation of PGES in skin xenografts and lymph nodes.

Keyword: Adipose-derived stem cells; Skin xenograft; Transplantation; Immunology

Student Number: 2019-35393

Parts of these thesis were previously published in *Transplant Proc*. 2022;54(8):2388-2395.

Table of Contents

Chapter 1. Immunomodulatory effect of ADSCs in human-to-mouse skin xenograft model

1.1. Introduction

Skin grafting has been widely used for the reconstruction of tissue loss caused by burns, trauma, or cancer. The insufficient supply of human tissues for autologous and allogeneic transplantations has attracted interests in xenogeneic transplantation as an alternative donor source (1). However, the success rate of non-autologous skin transplantation is relatively poor compared with that of other vascularized solid organs (2). In particular, xenograft rejection is more severe than allograft rejection (3, 4). Despite recent advances in surgery, immunology, and genetic engineering, skin xenografts have been considered temporary wound dressings that provide a better environment for subsequent autologous skin grafting (5). To date, cell-mediated acute rejection of skin xenografts has been a major immunological challenge with the current standard immunosuppressive therapy (6-8).

Increasing evidence indicates that mesenchymal stem cells (MSCs) have immunomodulatory effects in the treatment of various diseases such as graft-versus-host disease (9). Previous reports have shown that MSCs regulate innate and adaptive immune responses via cell-to-cell contact and through the paracrine secretion of soluble factors (10). The capability of MSCs to modulate the activity of T cells (9, 11, 12), B cells (13, 14), macrophages (15), natural killer (NK) cells (13), and dendritic cells (DC) (16) has been documented in numerous studies (17). MSCs also secrete several soluble factors that mediate immunomodulation, including prostaglandin E2 (PGE2) (18, 19), indoleamine-pyrrole 2,3-dioxygenase (IDO) (20),

and nitric oxide (21).

Adipose-derived stem cells (ADSCs) have more potent inhibitory effects on activated T cell proliferation than bone marrow and cord blood-derived MSCs. In addition, they are easier to obtain from human tissues (22, 23). Previous studies have demonstrated that ADSCs can promote tolerance induction in murine skin allograft transplantation models (24-26). Following revascularization, acute rejection of the transplanted skin tissue is primarily mediated by T cells (27, 28). ADSCs alleviate rejection of skin allografts by inhibiting the expression of proinflammatory cytokines and inducing regulatory T cells (24, 26, 29-32). However, the exact underlying mechanism remains unclear.

The aim of this study was to evaluate the immunosuppressive potential of ADSCs in xenogeneic transplantation of human skin onto immunocompetent rodents by comparing intravenous (IV) and subcutaneous (SC) injections of ADSCs in a human-to-mouse skin xenograft model.

1.2. Method

1.2.1. Animals and Study Design

All animal experiments were approved by the Institutional Animal Care and Use Committee of the Seoul National University Hospital (SNUH-IACUC; No. 21-0143-S1A0). Thirty male C57BL/6 mice weighing approximately 25 to 30 g each were divided into control, IV, and SC injection groups.

1.2.2. ADSC preparation and characterization

For localization of post-administration ADSCs, C57BL/6 transgenic mice

that express green fluorescent protein (GFP) were used. The inguinal fat pads were minced, washed, and digested with 0.2% type I collagenase (Sigma-Aldrich, St. Louis, MO) for 1 h at 37°C while shaking. Next, the collagenase was neutralized with Dulbecco's modified Eagle's medium (DMEM; Invitrogen, Carlsbad, CA) with 10% fetal bovine serum (FBS; Gibco, Life Technologies, Grand Island, NY) and 1% penicillin-streptomycin (Gibco). After centrifugation, the suspension was filtered through a 100-μm strainer. Filtrates were then centrifuged at 400 g for 5 min. The pellet was resuspended in the same complete medium. These cells were plated in 10-cm culture dish and maintained at 37°C in 5% CO2 and 95% humidity. When the cells reached >80% confluence, the adherent cells were disassociated with 0.05% trypsin-EDTA (Sigma-Aldrich) and re-plated. Third-passage cells were used in all the subsequent experiments.

The morphology of ADSCs was observed under a light microscope (Olympus IX71, Tokyo, Japan). The immunophenotypes of the ADSCs were determined by the expression of surface markers [anti-CD34 (ab81289; Abcam, Cambridge, UK) and CD11b (ab10558; Abcam) as hematopoietic lineage markers and anti-CD73 (ab181469; Abcam) and CD90 (ab107595; Abcam) as mesenchymal cell lineage markers] was analyzed using a flow cytometer (BD FACSymphony A3, Franklin Lakes, NJ).

1.2.3. Skin transplantation model

Informed consent was waived after approval by the Institutional Review Board of Seoul National University Hospital (No. 2021-3273), and the skin was harvested from the remnants of the transverse rectus abdominis musculocutaneous (TRAM) flap in patients with breast cancer who underwent breast reconstruction

after mastectomy. Human skin was used for the experiments within 3 days of collection. After removing the subcutaneous tissue with scissors, 1 x 1 cm^2-sized full-thickness skin xenografts were transplanted onto the same sized skin defect on the backs of B6 mice and fixed with simple interrupted stitches.

1.2.4. Injection of ADSCs

To determine whether ADSCs could improve skin xenograft survival, third-passage ADSCs were injected intravenously through the tail vein (IV group) or locally at 10 sites into the subcutaneous plane of the recipient bed (SC group) using a 1-mL insulin syringe. The SC and IV groups received ADSCs (1 mL) at a concentration of 1.0×10^6 cells per mouse.

1.2.5. Skin Graft Survival Assessment

The surface area of the survived-looking graft was measured on days 0, 1, 2, 3, 5, 7, 10, and 14 using ImageJ software (National Institutes of Health, Bethesda, MD, USA). Skin graft survival rates were expressed as a ratio of its original size on day 0.

1.2.6. In Vivo Imaging System

GFP-labelled ADSCs were monitored using an in vivo imaging system instrument (IVIS Imaging System Series 200, Caliper Life Science, Hopkinton, MA, USA) on days 0, 1, 2, 3, 5, 7, 10, and 14 after injection.

1.2.7. Histologic Examination

Samples from the skin grafts were fixed with 4% paraformaldehyde overnight. The paraffin-embedded tissue was then sectioned at a thickness of 4 μm and stained with hematoxylin and eosin. Histopathology was assessed by a single pathologist according to the degree of tissue destruction vs intact tissue alignment, infiltration of inflammatory cells, epidermal thickness, and extent of necrosis and fibrosis revealed by hematoxylin and eosin staining. Inflammation severity was graded on a 3-point scale as follows: 0 = absent, 1 = mild (<25%), 2 = moderate (25% to 75%), and 3 = severe (>75%).

The expression of immune cell markers in the tissue samples was examined by immunohistochemistry (IHC). Samples were incubated with following antibodies at 4°C for overnight: anti-FOXP3 antibody (1:100 dilution; eBioscience, San Diego, USA), anti-CD4 antibody (1:1000 dilution; Abcam), anti-CD8 antibody (1:1000 dilution; Abcam), and anti-NK1.1 antibody (1:100 dilution, Novusbio, Colorada, USA). Semiquantitative analysis was performed by measuring the proportion of the positively stained area in five random fields.

1.3. Results

1.3.1. Examination Characterization of mouse ADSCs

Cultured cells were plastic-adherent and exhibited a spindle-shaped morphology when observed under a light microscope. Flow cytometry analysis revealed that the cultured cells did not express hematopoietic markers (CD34 and CD45), whereas they expressed mesenchymal stem cell markers (CD90 and CD105; **Figure 1**).

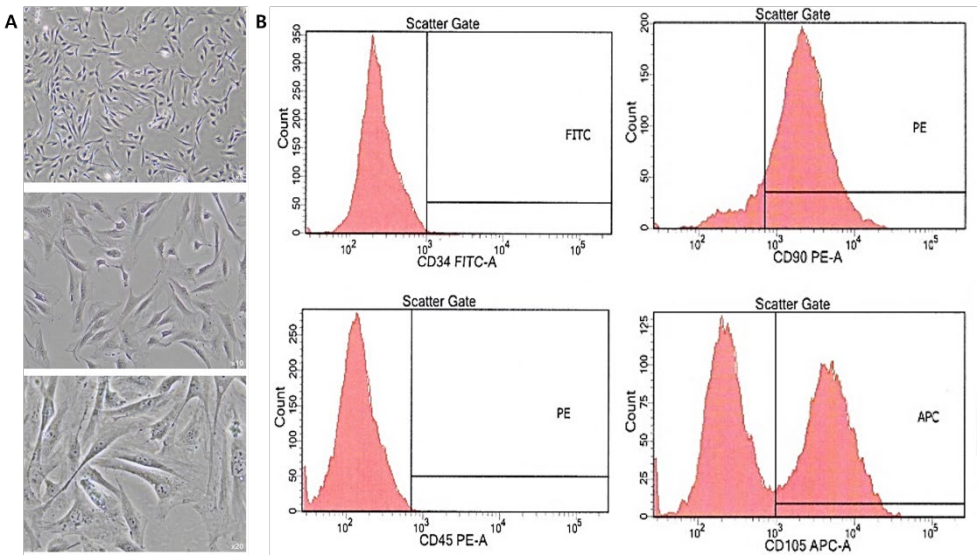

Figure 1. Identification of mouse adipose-derived stem cells. (A) Morphology of mouse adipose-derived stem cells at passage 3, observed via microscopy with magnification of 5, 10, and 20 times (first, second, and third row, respectively). ADSCs were plastic-adherent when maintained in standard culture conditions. (B) Flow cytometry analysis for surface markers at passage 3 before transplantation. Cultured cells did not express CD34 or CD45, whereas they expressed CD90 and CD105.

1.3.2. Distribution of GFP-labelled ADSCs After Administration

Bioluminescent imaging showed that GFP-labeled ADSCs were concentrated on the skin graft during the study period in both IV and SC groups (**Figure 2**). The results indicated that systemically administered ADSCs were recruited to the grafted area.

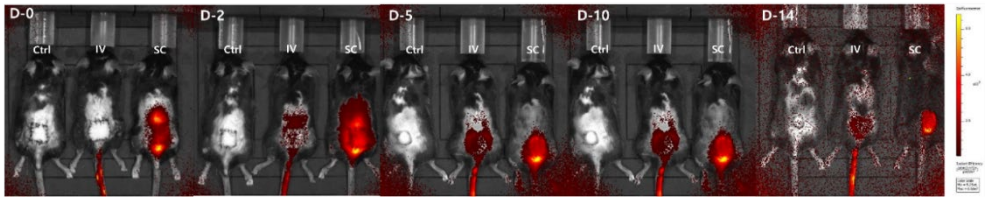

Figure 2. Bioluminescent imaging of mouse adipose-derived stem cells after intravenous and subcutaneous injection in C57BL/6 mice using an in vivo imaging system (Ctrl=control, IV=intravenous injection, and SC=subcutaneous injection).

1.3.3. Skin Graft Survival Assessment

Grafts were monitored for 14 days (on days 0, 1, 2, 3, 4, 5, 7, 10, and 14) after skin grafting (**Figure 3**). On day 14 after transplantation, mean 70 ± 4% of skin xenografts in the control group had detached from the recipient. However, SC injection of ADSCs significantly increased graft survival compared with the control group at 14 days after grafting (53 ± 3% vs 30 ± 4%, P = .02). The mean survival rate of the IV group was higher than that of the control group, which was not statistically significant (54% ± 8% vs 30% ± 4%, P = .06).

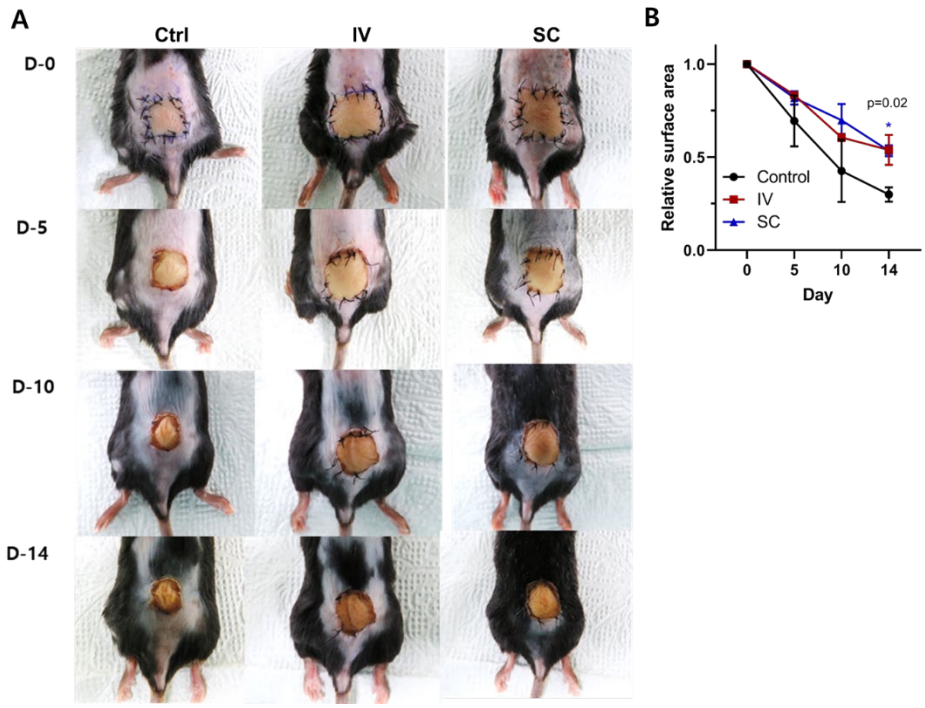

Figure 3. Skin graft survival assessment. (A) Representative photographs of xenogeneic skin grafted to mice on days 0, 5, 10, and 14 after grafting. (Ctrl=control, IV=intravenous injection, and SC=subcutaneous injection) (B) Survival graph after human full-thickness skin grafting to C57BL/6 mice that subsequently received intravenous and subcutaneous injections of mouse adipose-

derived stem cells. At 14 days after grafting, subcutaneous injection of ADSCs significantly increased skin graft survival compared with the control group (53±3% vs. 30±4%, p=0.02). (B)

1.3.4. Histological Examination

Histologic examinations were performed at 1 week after surgery (**Figure 4**). In terms of tissue destruction and inflammatory cell infiltration, inflammatory reactions were attenuated by ADSCs treatment ($P < .05$). Conversely, inflammatory responses in the IV group were inconsistent ($P > .05$). Epidermal thickness was greater in the SC group than in the IV group, but there was no significant difference between the IV and control groups. No necrosis or fibrosis was observed in the SC group.

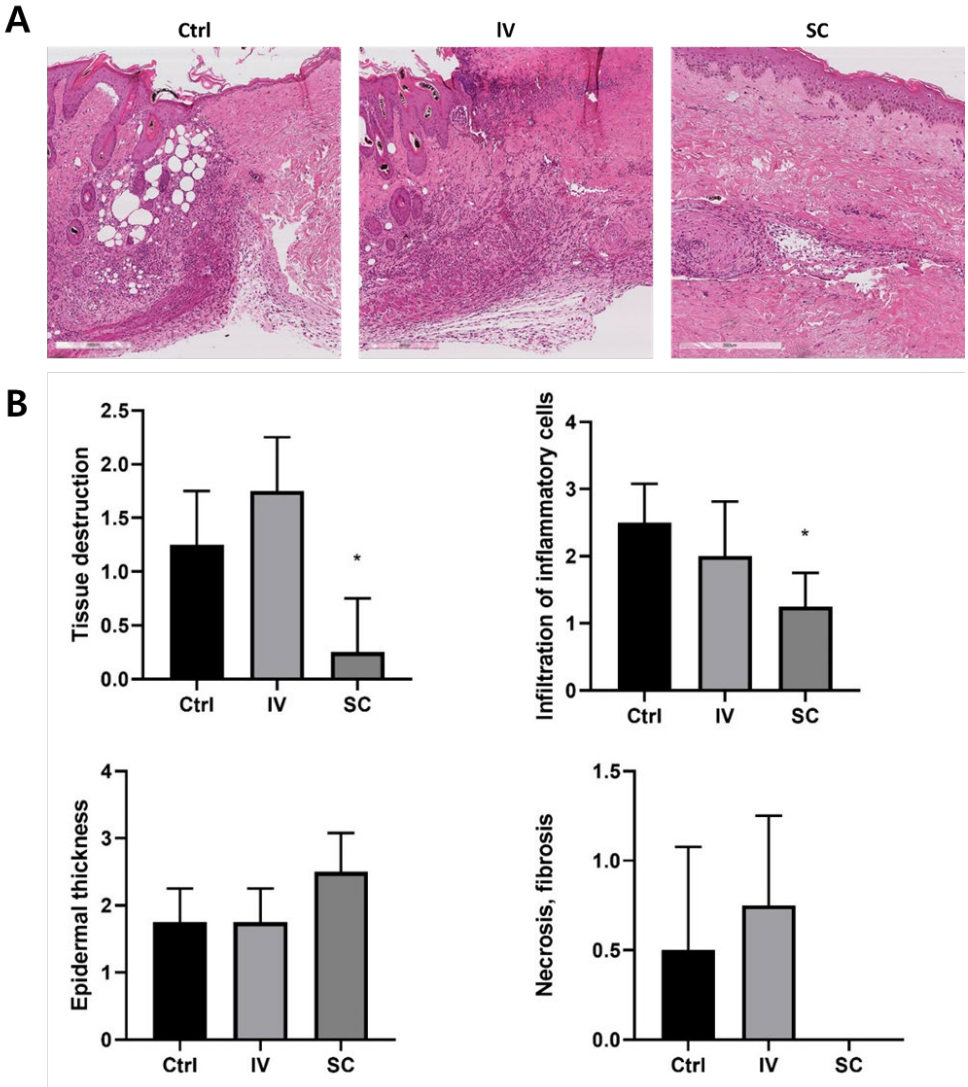

Figure 4. Histological findings of xenogeneic full-thickness skin graft 1 week after grafting. (Ctrl = control, IV = intravenous injection, and SC = subcutaneous injection). (A) Hematoxylin and eosin staining. The SC group showed less tissue destruction (derangement of fiber alignment), greater epidermal thickness, less infiltration of inflammatory cells, and no necrosis or fibrosis compared with the control group. (B) Histology score examination revealed a smaller inflammatory response in the SC group than in the control group. Asterisk denotes statistical difference at a $P < 0.05$ level of significance.

IHC revealed relative decreases in the percentages of FOXP3^{+}, CD4^{+}, CD8^{+}, and NK1.1 cells in the IV and SC groups compared with the control group (**Figure 5**). The proportion of the positively stained area in the epidermis and dermis were presented as mean values: FOXP3 (control: 3%, IV: 1%, SC: 1%), CD4 (control: 10%, IV: 1%, SC: 1%), CD8 (control: 15%, IV: 10%, SC: 3%), NK1.1 (control: 30%, IV: 20%, SC: 10%).

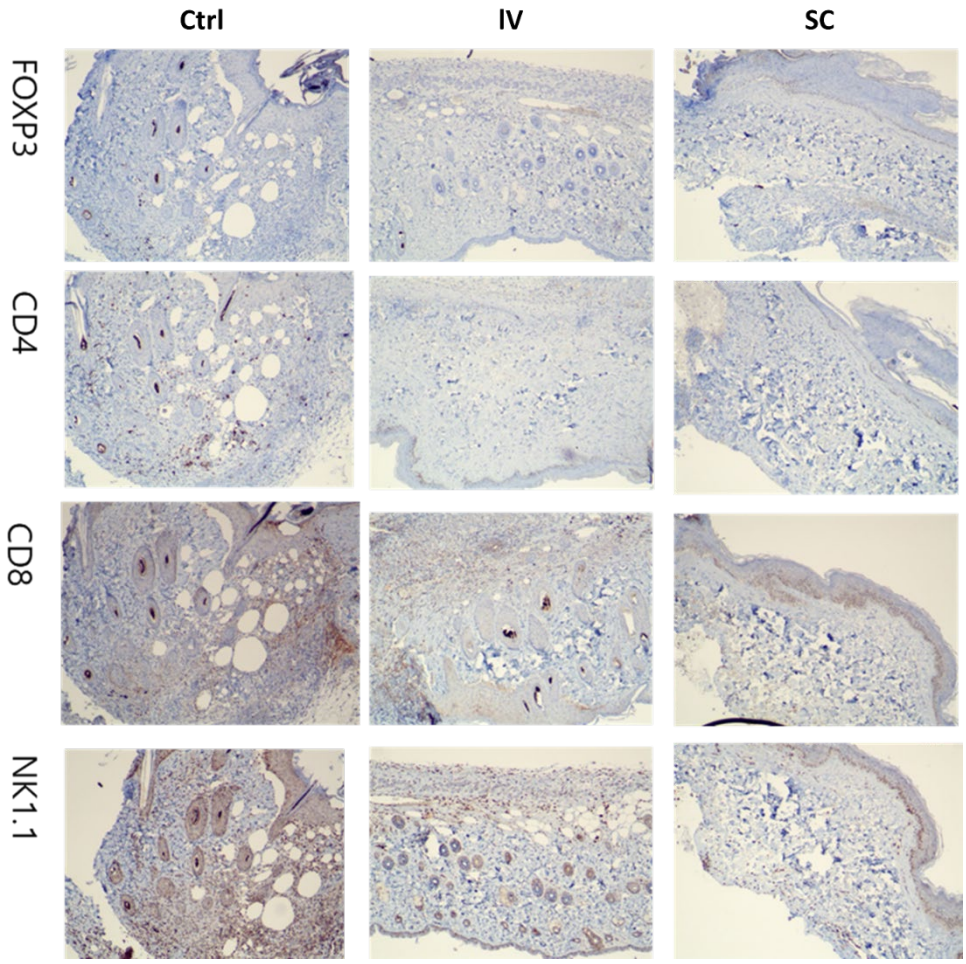

Figure 5. Representative images of immunohistochemistry analysis (IHC). Relative decreases in the percentages of FOXP3+, CD4+, CD8+, and NK1.1+ cells in the IV and SC group, compared with the control group was observed. (Ctrl = control, IV = intravenous injection, and SC = subcutaneous injection)

1.4. Discussion

The results showed that ADSCs significantly reduced rejection responses, leading to improved skin xenograft survival. The skin xenotransplantation evokes strong immune responses(29). In general, acute rejection occurs within 10-20 days without immunosuppression. The skin graft becomes vascularized within a few days, such that host T cells are activated through antigen-presenting cells (29). Graft rejection is mediated by both the innate and adaptive immune system (33). In this study, histological examination revealed a significant decrease in the inflammatory responses between the SC and control groups at 1 week postoperatively, before considerable macroscopic changes were noted. In addition, IHC revealed decreased numbers of $CD4^+$ and $CD8^+$ cells in the SC group at postoperative 1 week, compared with the control group. These results are consistent with the findings of previous studies in which ADSCs demonstrated immunosuppressive effects by suppressing overall T-cell proliferation (34-36)

Furthermore, whether administration routes influenced the immunomodulatory effect of ADSCs was tested. The data showed that the SC injection of ADSCs was superior for inducing immunosuppression and promoting xenograft survival compared with the IV injection method. Local injections may offer more opportunities for cell-to-cell contact and paracrine signaling(37). In contrast, the therapeutic potential of IV injections of ADSCs is associated with the paracrine release of cytokines and growth factors. In a previous study, methods of application (intravenous, intramuscular, and topical) were compared in terms of wound healing in a rodent full-thickness wound defect model; no significant differences were found(38). Similarly, Hu et al. reported that ADSCs increased the survival of skin allografts in mice regardless of local or systemic injection.

There is increasing evidence on the homing effect of ADSCs to sites of inflammation (39, 40). Consistent with previous studies, it was observed that ADSCs were concentrated in the grafted area immediately after administration(41). The homing effect of ADSCs appeared to persist during rejection reaction.

This experiment had several limitations. First, the study period was comparatively short in terms of observing graft survival. Second, our analysis of the involved T-cell subtypes and related cytokine profiles was limited. Further studies over a longer time period are necessary to investigate the underlying immunomodulatory mechanisms of ADSCs with respect to skin graft survival in a skin xenotransplantation model.

In conclusion, the findings indicate that the subcutaneous injection of ADSCs enhances xenograft survival in a mouse skin transplantation model. Furthermore, subcutaneous injection appears to be superior to intravenous injection in terms of skin graft survival.

Chapter 2. Multiple injections of ADSCs for human-to-rat skin xenograft survival via immune modulation

2.1. Introduction

Despite the documented immunosuppressive capacities of MSCs, some clinical studies have shown minimal effects of MSCs on graft rejection (17, 42). This suggests that repeated administration of ADSC may be required for a desirable therapeutic effect (43, 44). Several studies have examined the efficacy of repeated MSC injections in spinal cord injury (45), osteoarthritis (46), vascularized composite allotransplantation (47), and burn wounds (48). However, there is a lack of studies on whether repetitive injections of ADSCs into skin xenografts are beneficial.

The aim of this experiment was to compare the immunomodulatory effects of single and triple local injections of ADSCs, and in xenogeneic transplantation of human skin onto immunocompetent rats. In the present study, skin grafts, four times (4 cm^2 versus 1 cm^2) the size used in the preliminary study, were transplanted in a rat model to effectively deliver ADSCs by local injection. For repeated administrations, ADSCs were injected into the subcutaneous planes of the rat skin that was in contact with the xenograft, rather than into the graft itself or into the fascial layer of the graft bed, as in previous studies (30, 32, 49). As skin xenografts become inflamed by POD 7-9 and fully rejected by POD 8-12, repeated doses of ADSCs were administered within 5 days to effectively suppress the immune response (46, 50).

2.2. Methods

2.2.1. Animals and Study Design

All animal experiments were approved by the Institutional Animal Care and Use Committee of the Seoul National University Hospital (SNUH-IACUC; No. 21-0143-S1A0). 6-8-week-old male Sprague-Dawley (SD) rats (220–250 g) were purchased from Koatech (Pyeongtaek, Republic of Korea). Three groups (n = 21 in each group) were compared in this study: triple injections of phosphate-buffered saline (PBS group), and triple injections of ADSCs (ADSC × 3 group) at post-operative days (POD) 0, 3, and 5. Rats were randomly assigned to each experimental group. The PBS group received three injections of 1 mL PBS. The ADSC × 1 group received one injection of 1×10^6 ADSCs suspended in 1 mL of PBS and 2 injections of 1 mL PBS. The ADSC × 3 group received three injections of 1×10^6 ADSCs suspended in 1 mL of PBS. Rats in each group were divided into four subgroups and sacrificed for further analyses at POD 14.

2.2.2. ADSC preparation and characterization

The rat ADSCs were prepared using the same method described above. The immunophenotypes of the ADSCs were determined by the expression of surface markers [anti-CD34 (ab81289; Abcam, Cambridge, UK) and CD11b (ab10558; Abcam) as hematopoietic lineage markers and anti-CD73 (ab181469; Abcam) and CD90 (ab107595; Abcam) as mesenchymal cell lineage markers] was analyzed using a flow cytometer (BD FACSymphony A3, Franklin Lakes, NJ).

2.2.3. Skin transplantation model

Skin grafting was performed as described above. The 2 x 2 cm^2-sized full-thickness human skin was transplanted onto the same sized skin defect on the backs of rats and fixed with 4-0 interrupted silk sutures. For the compressive tie-on dressing, a bolster of cotton gauze impregnated with betadine was applied to the skin xenografts for 7 days.

For the compressive tie-on dressing, a bolster of cotton gauze impregnated with betadine was applied to the skin xenografts for 7 days. The first inspection was performed on POD 7 after removal of the tie-on dressing, followed by POD 10 and 14, and weekly thereafter until POD 56. Rats were sacrificed on POD 7, 10, 14 for subsequent analysis (n = 6 per subgroup); and on POD 56 for long-term observation (n = 3 per subgroup).

Skin discoloration, sloughing, and dry scab formation on inspection and palpation were examined to determine xenograft rejection. Photographs of skin xenografts were taken at close and fixed distances. The surface area of the xenografts was measured using the ImageJ software (NIH, Bethesda, MD). The relative surface area was expressed as a percentage of the size on POD 7 (when the tie-on dressing was removed) and plotted against time. Samples (skin xenografts, axillary lymph nodes, and blood) were collected and analyzed using subsequent methods.

2.2.4. Injection of ADSCs

Respective administration of ADSCs was subcutaneously administered evenly at eight different points on the rat skin in contact with the xenograft (covered with the tie-on dressing) using a 1-mL insulin syringe with a 30 G needle.

Finally, a self-adherent bandage is used to cover the tie-on dressing.

2.2.5. Histological Examination

Skin xenograft samples were fixed overnight with 4% paraformaldehyde and embedded in paraffin wax. Paraffin-embedded tissues were sectioned at a thickness of 4 μm. Sections were deparaffinized and stained with hematoxylin and eosin (H&E) and Masson's trichrome (MT).

The degree of graft rejection was assessed using the Banff 2007 pathomorphological classification of H&E-stained sections (51). The analysis included the occurrence of apoptosis, dyskeratosis, necrosis in the epidermis, lymphocytic infiltrates around the blood vessels, and appendages within the graft. Images were randomly assigned for blind grading and evaluated by two different examiners separately.

2.2.6. Immunohistochemistry (IHC)

The deparaffinized slides were incubated with primary antibodies [anti-rat/human proliferating cell nuclear antigen (PCNA; 1:100; ab29; Abcam, Boston, MA, USA), anti-rat CD31 (1:200; GTX130274; GeneTex), anti-rat collagen 1A1 (1:125; sc-293182; Santa Cruz Biotechnology, Dallas, TX), anti-rat collagen 3A1 (1:250; sc-271249; Santa Cruz Biotechnology), anti-rat/human CD3 (1:200; ab5690; Abcam), anti-rat CD4 (1:50; ab237722; Abcam), anti-rat CD8 (1:150; GTX41830; GeneTex), anti-rat CD68 (1:200; ab125212; Abcam), and anti-rat/human IFN-γ (1:125; GTX66714; GeneTex)]. After washing with PBS, the slides were incubated with appropriate secondary antibodies. The slides were developed using DAB and counterstained with hematoxylin. Ventana Chromo

Map Kit (Ventana Medical Systems) was used for detection.

To quantify cell counts, an immunoreactive scoring (IRS) system was used in at least three microscopic fields per section in six subjects per subgroup to examine the expression of PCNA (in the epidermis of the xenografts), CD3, CD4, CD8, CD68, and IFN-γ (within the xenografts in contact with the rat tissue), IRS (0-12) was calculated as the staining intensity (negative, 0; weakly positive, 1; moderately positive, 2; strongly positive, 3) multiplied by the proportion of positive cells (negative: 0, <10%, 1;10-50%, 2; 51-80%, 3, >80%; 4).

For vascularization, the number and area of CD31-positive blood vessels were measured using ImageJ. Only blood vessels with diameters of 2–10 μm were counted (52). For collagen deposition, the area of collagen 1A1- and 3A1-positive fibrils was measured, and the collagen type 1/3 ratio was calculated for comparison. All images were digitized at 640 × 480 or 1280 × 960 pixel resolutions (magnification × 400 and × 200, respectively).

2.2.7. Real-time quantitative real-time polymerase chain reaction (RT-qPCR)

Total RNA was isolated from human skin grafts and rat axillary lymph nodes using the TRIzol reagent (Invitrogen). The extracted RNA was reverse-transcribed into cDNA using the ReverTra Ace qPCR RT Master Mix (Toyobo, Osaka, Japan). PCR was conducted using SYBR Green PCR Master Mix (Toyobo) and QuantStudio 5 (Applied Biosystems, Foster City, CA). The primer sequences used are listed in **Table 1**. The results were presented using the comparative CT method, relative to an internal control gene (Tbp).

Gene		Sequence (5'->3')
Ifng	Forward	TGAAAGACAACCAGGCCATC
	Reverse	AGCTTTGTGCTGGATCTGTG
Ptges	Forward	TGTGAGGACCACGAGGAAATG
	Reverse	CGCAACGACATGGAGACGAT
Tbp	Forward	AAGGGAGAATCATGGACCAG
	Reverse	CCGTAAGGCATCATTGGACT

Table 1. Primer sequences used for quantitative real-time PCR

2.2.8. Enzyme-linked immunosorbent assay (ELISA)

The serum was prepared by allowing whole blood to clot at 20°C and centrifuging at 1,000 × g for 10 min. After removing the clot, the supernatant was stored at -80°C. Serum IFN-γ levels were measured using an ELISA Kit (RTFI01244, AssayGenie, Windsor Place, Dublin, Ireland) according to the manufacturer's instructions.

2.2.9. Western blotting (WB)

Skin graft samples were collected from the transplanted rats and snap-frozen in liquid nitrogen. The tissues were chopped and homogenized with a TissueRuptor II (Qiagen, Hilden, Germany) and lysed in SDS sample loading buffer (Sigma). The samples were subjected to SDS-PAGE and subsequently transferred to Immobilon-P PVDF membranes (Merck, Rahway, NJ). Transferred membrane proteins were probed with the indicated primary antibodies [anti-PGES (sc-365844; Santa Cruz Biotechnology); anti-β-tubulin (sc-5274; Santa Cruz Biotechnology)] and incubated on a rocker for overnight at 4°C. HRP-conjugated secondary antibodies (Cell Signaling Technology, Danvers, MA) were applied to the membranes and visualized with chemiluminescence reagents (GenDEPOT,

Katy, TX).

2.2.10. Statistical analysis

Data are presented as the mean ± standard deviation. After the assumption of normality was tested, non-parametric one-way ANOVA with multiple comparison test was used in this study. All results were analyzed and graphed using GraphPad Prism 8.0 (GraphPad Software, La Jolla, CA). Differences were considered statistically significant at $p < 0.05$.

2.3. Results

2.3.1. Characterization of rat ADSCs

The cultured ADSCs were plastic-adherent and showed a normal spindle-shaped morphology (**Figure 6A**). Flow cytometry analysis revealed that the cells were positive for mesenchymal lineage markers (CD73 and CD90) and negative for hematopoietic lineage markers (CD11b and CD34) (**Figure 6B**). These findings confirmed the characterization of the ADSCs.

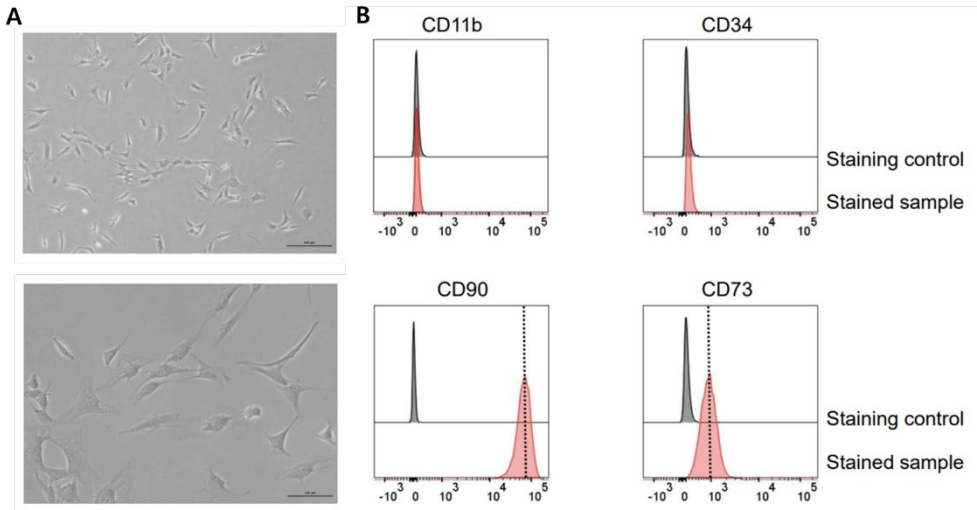

Figure 6. Characterization of adipose-derived stem cells. (A) Representative images of cell morphology under light microscope. Lower (left) and higher (right) magnification. Scale bar, 100 μm. (B) Flow cytometric analysis for mesenchymal (CD73 and CD90) and hematopoietic (CD11b and CD34) cell markers.

2.3.2. Delayed macroscopic rejections of skin xenografts by ADSCs

Rats were transplanted with human skin xenografts, and PBS or ADSCs were subcutaneously administrated at four different timepoints (**Figure 7A**). Representative images of xenografts on POD 7, 10, and 14 are shown in Figure 7B. The PBS group displayed sloughing followed by dry scab formation within 7-10 days, which was earlier than that in the ADSC × 3 group (within 14-21 days) (**Figure 7B**).

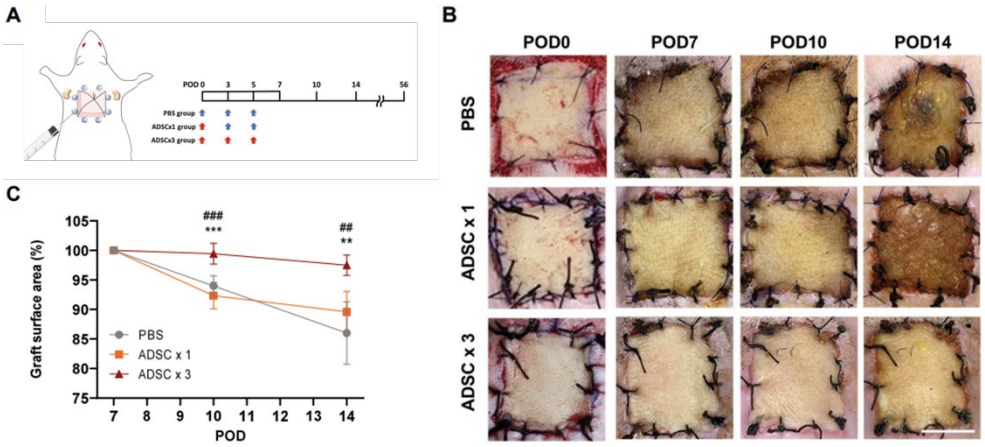

Figure 7. Study design and macroscopic findings of human skin xenografts. (A) Rats were randomized into three groups: PBS, ADSC × 1, and ADSC × 3 groups (n = 21 per group). Each 1 ml of PBS and/or ADSCs suspended in PBS was locally injected on POD 0, 3, and 5. After the removal of the tie-on dressing on POD 7, rats were sacrificed on POD 7, 10, 14 for subsequent analysis (n = 6 per subgroup); and on POD 56 for long-term observation (n = 3 per subgroup). Blue arrows, PBS; red arrows, ADSCs (1 x 106 cells/ml). (B) Representative images of the skin xenografts of each group on POD 0, 7, 10, and 14. The ADSC × 3 group showed considerably delayed xenograft rejection compared to the ADSC × 1 group. (C) Quantitative evaluation of the relative surface area of the skin xenografts (n=6 per

group). Statistical analysis by two-way ANOVA. ***$p < 0.001$, **$p < 0.01$, compared to the PBS group. ###$p < 0.001$, ##$p < 0.01$, compared to the ADSC × 1 group. PBS, phosphate-buffered saline; ADSC, adipose-derived stem cell; POD, postoperative day.

In the ADSC × 3 group, the xenografts maintained a more viable skin color and soft texture on inspection and palpation until POD 14. Based on long-term observations (8 weeks), the early period (before POD 14) appeared to be critical for xenograft rejection. In the late period (after POD 14), most of the xenografts turned into dry scabs and firmly adhered to the rat skin in all three groups (**Figure 8**). The surface area in the ADSC × 3 group was significantly smaller than that of the other two groups on POD 10 and 14 ($p < 0.001$ and < 0.01, respectively; Figure 7C), which might be associated with the progression of graft rejection. Compared to the PBS group, the ADSC × 1 group showed no significant differences in the reduction of surface area. These results show that triple injections of ADSCs effectively prolonged the survival of skin grafts.

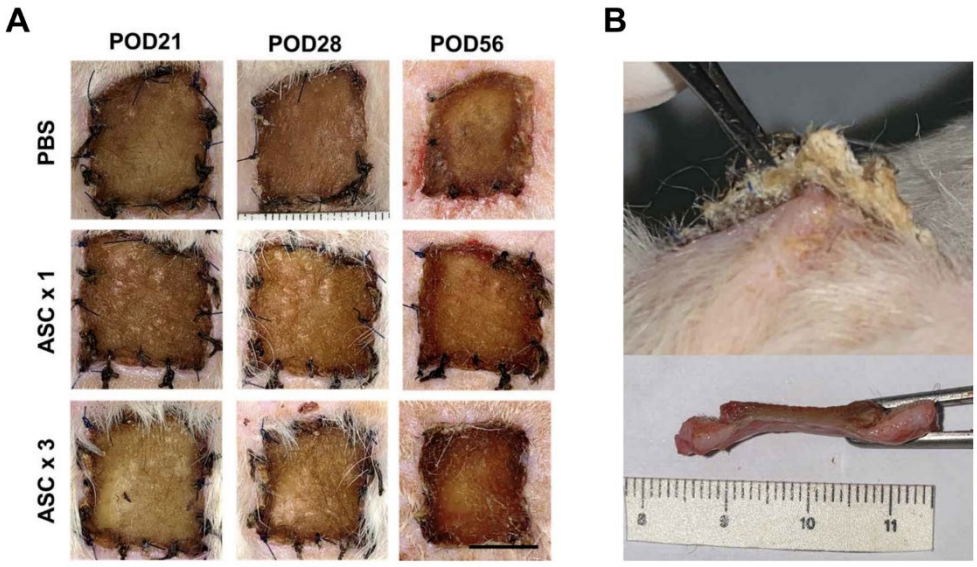

Figure 8. Long-term results of the skin xenografts until postoperative 8 weeks. (A) Representative images of the xenografts on POD 21, 28 and 56. Scale bar, 1 mm. (B) The human skin xenografts firmly attached to the rat tissue as dry scabs 8 weeks post operation.

2.3.3. Histopathological analysis of reduced graft rejection by ADSC

Histopathological examinations revealed that local injections of ADSCs lowered the Banff scores on POD 7, 10, and 14 in a dose-dependent manner (**Figures 9A and B**).

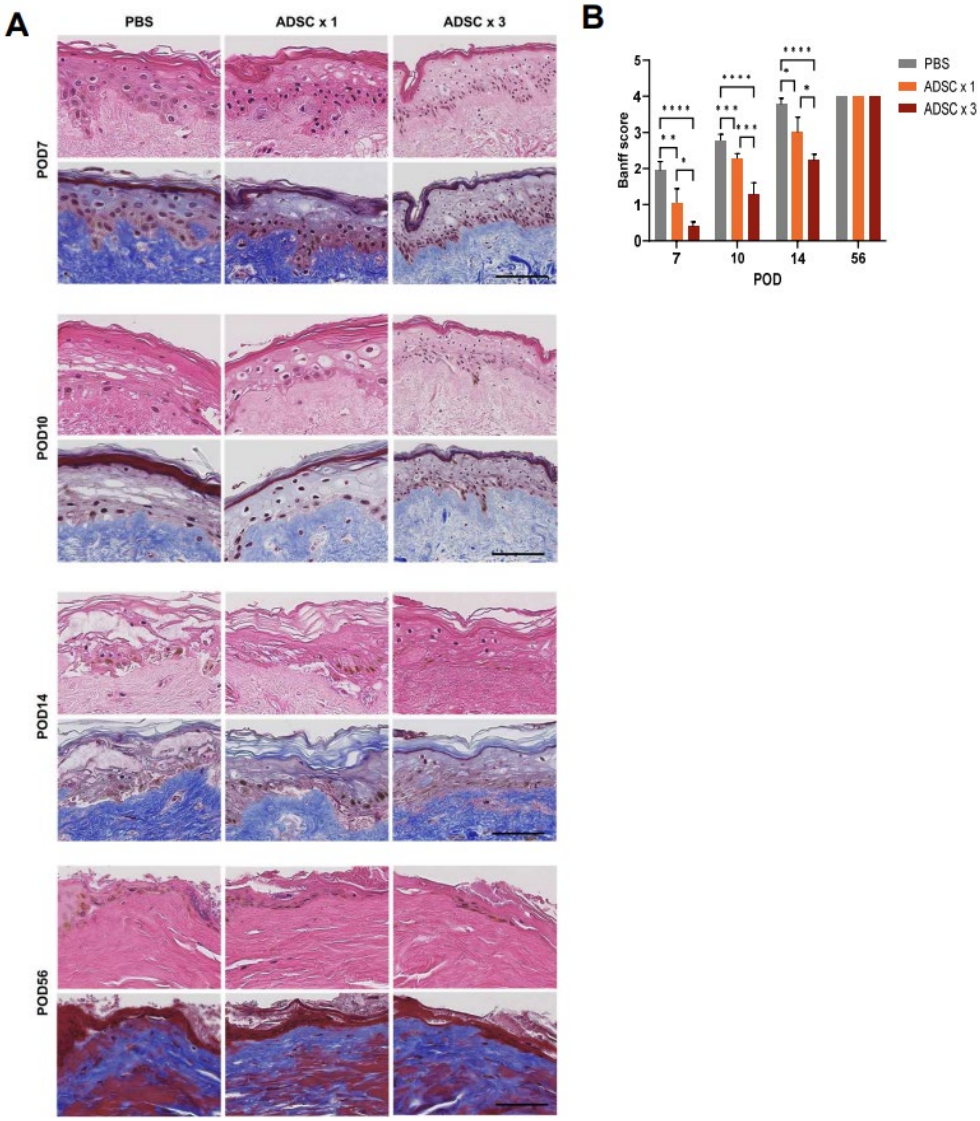

Figure 9. Histopathology of human skin xenografts. Representative images of hematoxylin and eosin (H&E) and Masson's trichome (MT) staining on POD 7, 10, 14, and 56. Scale bar, 50 μm. (B) Assessment of skin xenografts using the Banff classification (0-4). Statistical analysis by two-way ANOVA. ****$p < 0.0001$; ***$p < 0.001$; **$p < 0.01$; *$p < 0.05$; ns: not significant. PBS, phosphate-buffered saline; ADSC, adipose-derived stem cell; POD, postoperative day.

In the PBS group, notable epidermal apoptosis was observed on POD 10, eventually leading to flank necrosis on POD 14. On POD 56, H&E and MT staining showed nearly complete desiccation of the grafts in all groups (**Figure 10A**). The majority of xenografts were attached to the fibrotic graft bed, whereas regeneration of the rat-derived epithelium was limited to the peripheral rim of the xenografts (**Figure 10B**).

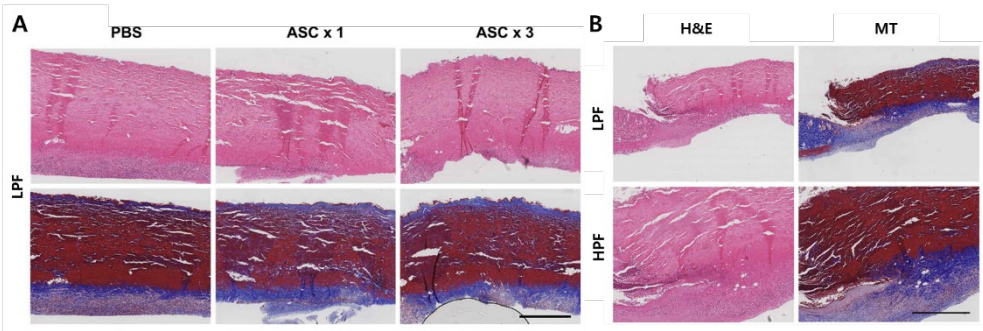

Figure 10. Long-term histological results of the skin xenografts until 8 weeks. (A) Representative images of hematoxylin and eosin (H&E) and Masson's trichome (MT) staining in low-power field (LPF) 8 weeks post operation. Scale bar, 1 mm. (B) Representative images showing the contact layer between the human xenograft and rat tissue 8 weeks post operation. Scale bar, 3 mm and 1 mm (for upper and lower row, respectively).

To delineate graft survival on POD 7, immunohistochemical (IHC) staining of proliferating cell nuclear antigen (PCNA) was performed. PCNA expression was observed in the basal cells of the epidermis of the skin xenografts. The number of PCNA-positive cells in the ADSC × 3 group was significantly higher than those in the PBS group on POD 7 ($p = 0.0003$; **Figures 11A and B**). PCNA-positive cells decreased with the advancement of rejection on POD 10 and 14 (**Figure 12**). In addition, IHC analysis showed that the area and number of CD31-positive blood vessels within the xenografts in contact with the rat tissue were significantly higher in the ADSC x3 group than in the PBS group on POD 14 ($p = 0.0004$ and 0.0386, respectively; **Figures 11C-E**). To evaluate collagen deposition during graft rejection, IHC analysis was performed to determine the expression of collagen types 1 and 3. It has been shown that decreased collagen 1 to 3 ratio in the transplanted skin graft reflects an early sign of the progression to graft rejection. Collagen type 1 is generally regarded as mature and rigid fibrils, whereas collagen type 3 is considered immature and thin. Data showed that Collagen type 1/3 protein expression ratio was significantly increased in the ADSC × 3 group on POD 14 compared to that in the PBS group ($p=0.0009$; **Figures 11F and G**). Overall, histopathological analysis showed that multiple ADSC injections had a positive effect on the markers, reflecting a reduction in skin rejection.

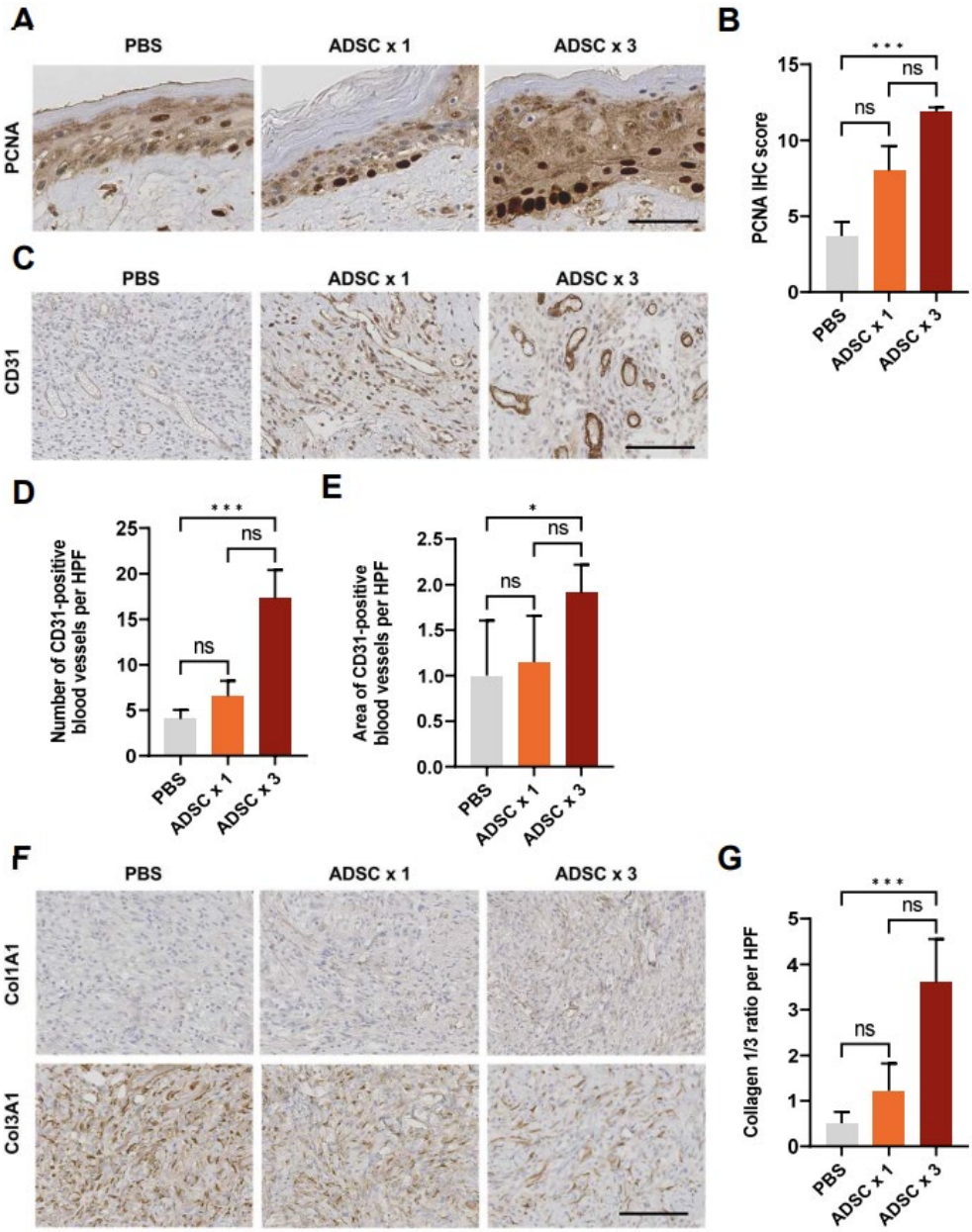

Figure 11. ADSCs significantly improved graft survival and vascularization.

(A) Representative images and (B) quantitation of IHC staining for proliferating cell nuclear antigen (PCNA) in the epithelium of the skin xenografts on POD 7 (n = 6 per group). Scale bar, 50 μm. (C) Representative images and (D, E) quantitation of IHC for CD31 on POD 14 (n = 6 per group). Scale bar, 100 μm. (F) Representative images and (G) quantitation of IHC for collagen type 1 and 3 on

POD 14 (n = 6 per group). Scale bar, 100 μm. Statistical analysis by one-way ANOVA. ***: $p < 0.001$; *: $p < 0.05$; ns: not significant. PBS, phosphate-buffered saline; ADSC, adipose-derived stem cell; POD, postoperative day; HPF, high-power field.

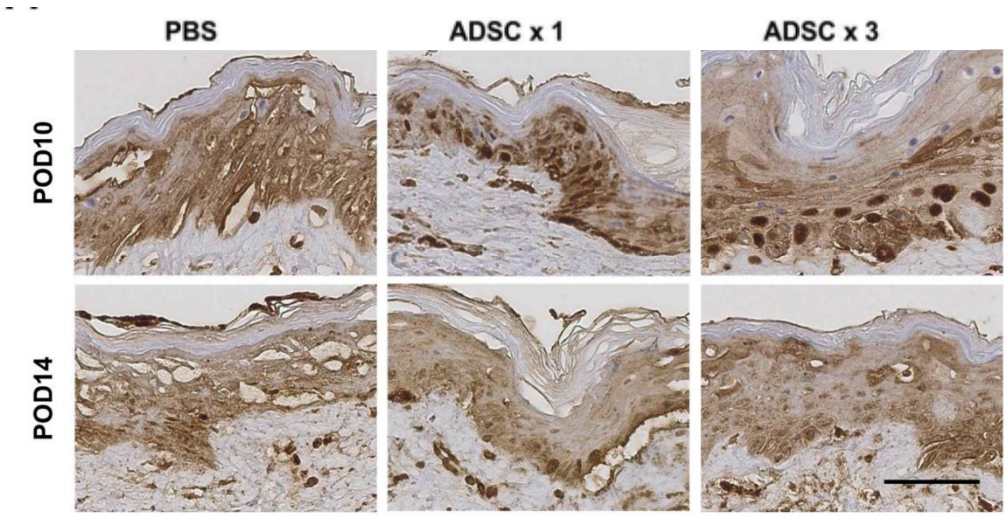

Figure 12. Immunohistochemistry staining for proliferating cell nuclear antigen (PCNA) in the epithelium of the skin xenografts on POD 10 and 14. Scale bar, 50 μm.

2.3.4. ADSCs inhibit the immune cell infiltration into xenografts

To evaluate cell-mediated rejection of xenografts, IHC staining of T cells and macrophages was performed. Once blood and lymphatic flows into the xenografts are established within 3-4 days, donor-derived antigen-presenting cells migrate to the skin-draining lymph nodes where they activate xenoreactive T cells (5, 56). In this study, substantial cellular infiltration of CD3-, CD4-, CD8-, and CD68-positive cells was observed with the advancement of xenograft rejection. Triple injections of ADSCs markedly inhibited the influx of T cells and macrophages into the xenografts on POD 7, 10, and 14 compared to the PBS and ADSC × 1 groups (**Figure 13**). However, the ADSC × 1 group had no significant differences in cellular infiltration compared to the PBS group on POD 14.

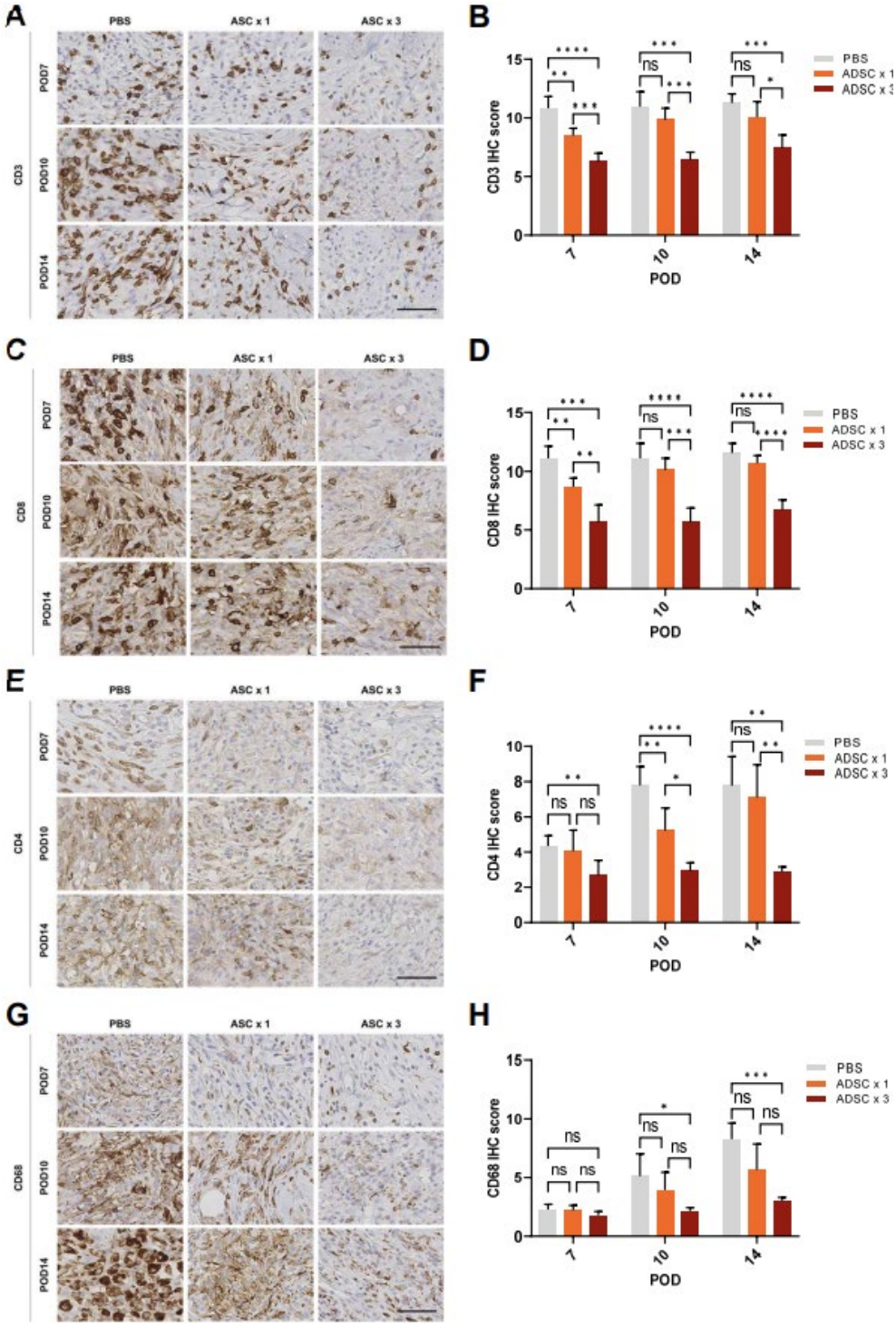

Figure 13. Immunohistochemical (IHC) analysis of immune cell markers. (A) Representative images and (B) quantitation of IHC for CD3 on POD 7, 10, and 14 (n = 6 per group). (C) Representative images and (D) quantitation of IHC for CD8

on POD 7, 10, and 14 (n = 6 per group). (E) Representative images and (F) quantitation of IHC for CD4 on POD 7, 10, and 14 (n = 6 per group). (G) Representative images and (H) quantitation of IHC for CD68 on POD 7, 10, and 14 (n = 6 per group). Scale bar, 50 μm. Statistical analysis by two-way ANOVA. ****: $p < 0.0001$; ***: $p < 0.001$; **: $p < 0.01$; *: $p < 0.05$; ns: not significant. PBS, phosphate-buffered saline; ADSC, adipose-derived stem cell; POD, postoperative day.

2.3.5. Downregulation of IFN-γ expression by multiple ADSC injection

As a key effector cytokine in the process of cell-mediated graft rejection, IFN-γ expression levels in skin xenografts, skin-draining axillary lymph nodes, and serum were measured at different time points and compared between the groups (57, 58). Ifng mRNA expression in skin xenografts was significantly lower in the ADSC × 3 group than in the PBS group on POD 14 ($p = 0.0319$), and than in the ADSC × 1 group on POD 10 and 14 ($p = 0.0095$ and 0.0141, respectively) (**Figures 14A**). Ifng mRNA expression in skin-draining axillary lymph nodes was significantly lower in the ADSC × 3 group than in the PBS group on POD 7 and 10 ($p = 0.0401$ and 0.0086, respectively), and in the ADSC × 1 group on POD 10 and 14 ($p = 0.0303$ and 0.0329, respectively) (**Figures 14B**). IHC analysis showed that the number of IFN-γ+ cells in the skin xenografts of the ADSC × 3 group was significantly lower than those in the PBS group on POD 14 ($p = 0.0004$) (**Figures 14C and D**). In addition, ELISA results showed that the concentration of IFN-γ protein in serum was significantly lower in the ADSC × 3 group than in the ADSC × 1 group on POD 14 ($p=0.0243$; Figure 14E). Taken together, triple injections of ADSCs downregulated IFN-γ expression, which correlated with reduced graft rejection.

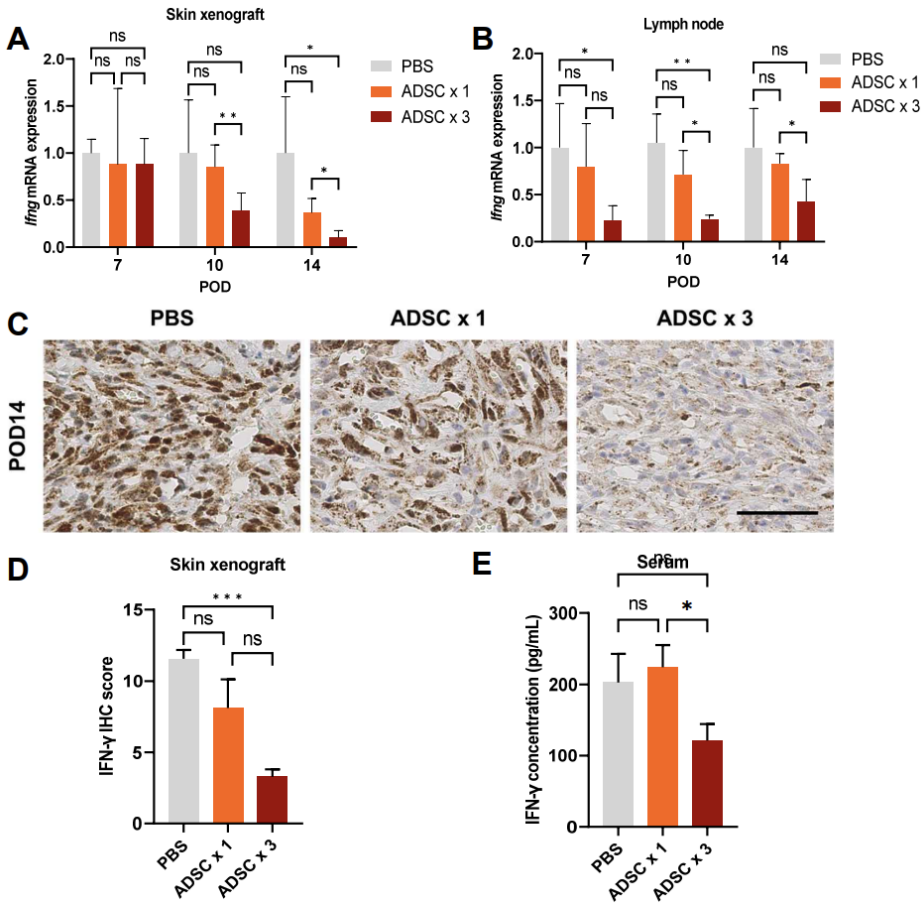

Figure 14. Downregulation of INF-γ expression levels in the skin xenografts, regional lymph nodes and serum. (A) Ifng mRNA expression in the skin xenografts on POD 7, 10, and 14 (n = 6 per group). (B) Ifng mRNA expression in the regional lymph nodes on POD 7, 10, and 14 (n = 6 per group). (C) Representative images and (D) quantitation of immunohistochemistry staining for INF-γ protein expression in the skin xenografts on POD 14 (n = 6 per group). Scale bar, 100 μm. (E) INF-γ protein concentrations in the serum on POD 14 (n = 4 per group). Statistical analysis by two-way ANOVA for (A, B), and one-way ANOVA for (D, E). ***: $p < 0.001$; **: $p < 0.01$; *: $p < 0.05$; ns: not significant. PBS, phosphate-buffered saline; ADSC, adipose-derived stem cell; POD, postoperative day; Ifng, IFN-γ, interferon gamma.

2.3.6. Upregulation of PGES expression by multiple ADSC injections

To investigate the immunosuppressive effects of ADSCs, the expression of prostaglandin E synthase (PGES) was analyzed. PGES is involved in the synthesis of prostaglandin E2 (PGE2), which exerts potent immunosuppressive actions (**Figure 15**). qPCR assay showed that Ptges mRNA expression in skin xenografts was higher than that in the PBS and ADSC × 1 groups on POD 10 and 14 (all $p < 0.05$) (**Figure 15A**). Ptges mRNA expression in skin-draining axillary lymph nodes was higher than that in the PBS and ADSC × 1 groups on POD 10 ($p = 0.0310$ and 0.0414, respectively; **Figure 15B**). Western blot analysis also showed that the protein levels of PGES in skin xenografts of the ADSC × 3 group were upregulated compared to those in the PBS group on POD 14 ($p = 0.0181$; **Figures 15C and D**). These results show that multiple injections of ADSCs increased the expression levels of PGES, which was negatively correlated with graft rejection.

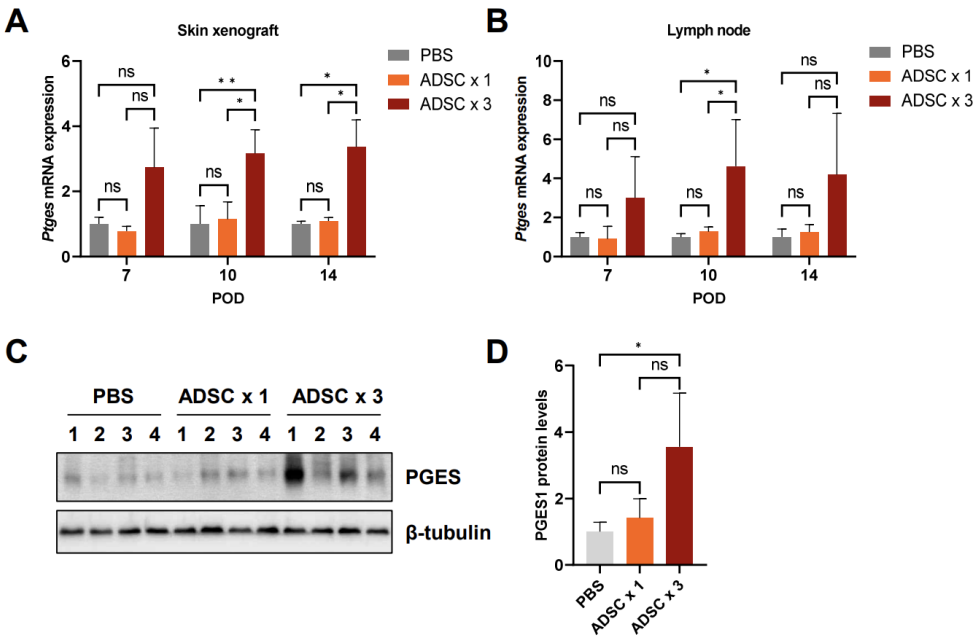

Figure 15. Upregulation of PGES expression levels in the skin xenografts and regional lymph. (A) Ptges mRNA expression in the skin xenografts (n = 6 per group). (B) Ptges mRNA expression in the regional lymph nodes (n = 6 per group). (C) Western blot analysis and (D) quantification of PGES protein levels in the skin xenografts (n = 4 per group). Full-length blots are presented in Additional file 7. Statistical analysis by two-way ANOVA for (A, B), and one-way ANOVA for (D). **: $p < 0.01$; *: $p < 0.05$; ns: not significant. PBS, phosphate-buffered saline; ADSC, adipose-derived stem cell; POD, postoperative day; PGES, prostaglandin E synthase.

2.4. Discussion

In this study, human skin xenografts were transplanted into naive SD rats to determine whether single or triple ADSC administration could exert functional immunosuppressive effects. Repeated injections of ADSCs were superior to single injections in inhibiting the cell-mediated rejection of xenografts. The data showed that the immunosuppressive effect of ADSCs increased with the injected dose. These findings were consistent with the dose-dependent inhibitory effects of ADSCs on T-cell proliferation in vitro (11, 53). Few studies have focused on the efficacy of multiple MSC injections (46-48, 54, 55). Most of them support that an additional dose potentiates the initial dose, which is not sufficient to improve the therapeutic outcomes of MSCs (46-48, 55). In this study, a single injection did not show significant differences in the macroscopic findings of xenograft rejection compared to the PBS group. One possible explanation for the need for multiple injections is that most MSCs might lose their proliferative capacity in the hostile microenvironment of the transplantation sites (48). Further studies are needed to enhance the proliferative potential and survival of intragrafted ADSCs.

In the majority of previous studies using the human skin xenograft model, human donor skin was transplanted into immunocompromised rodent hosts (59). One study showed that skin xenografts transplanted into athymic nude mice were tolerated indefinitely, showing the role of T cells in xenograft rejection (50). However, it is necessary to evaluate the immunomodulatory effects of ADSCs on skin xenografts in immunocompetent animals. In this study, these immunomodulatory effects of ADSCs appear to be associated with the downregulation of IFN-γ and upregulation of PGES (**Figure 16)**.

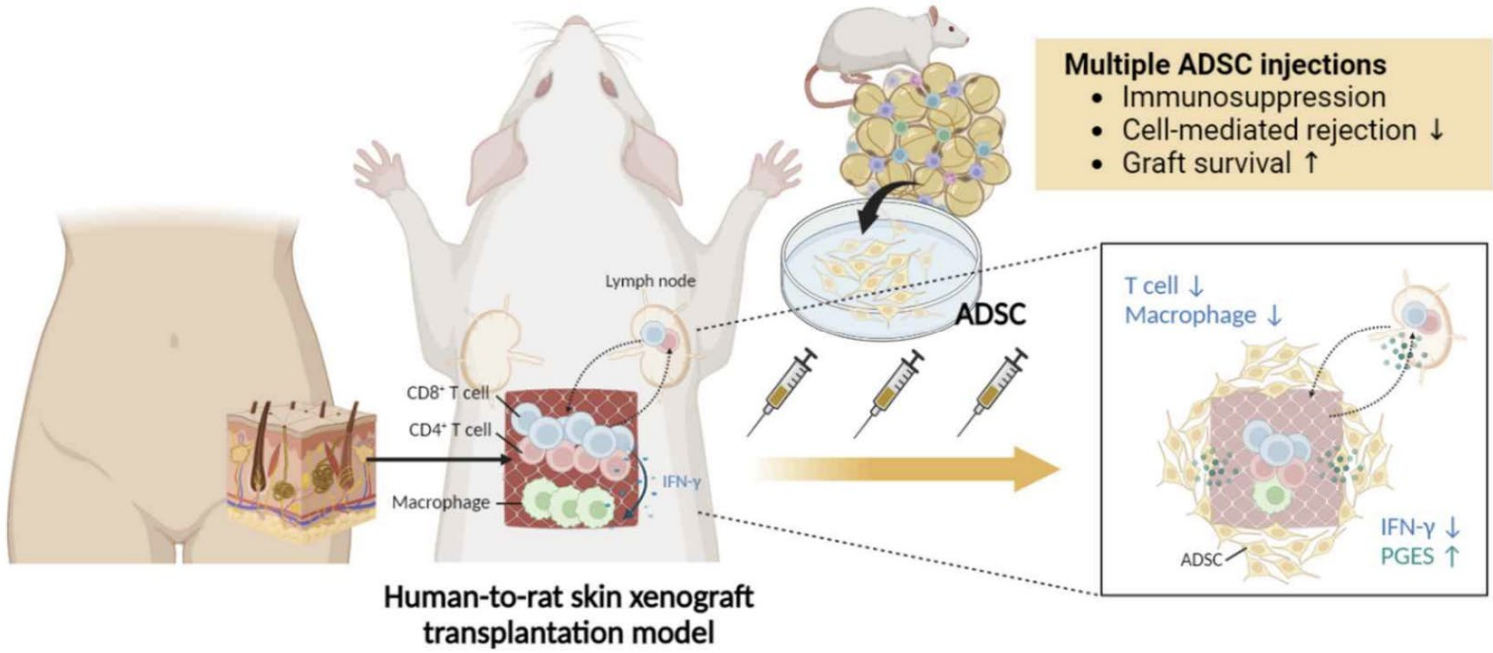

Figure 16. Proposed mechanisms of the immunomodulatory effects of ADSCs in human-to-rat skin xenotransplantation. Triple injections of ADSCs prolonged the survival of skin xenografts by modulating T cell proliferation and macrophage activation, which was associated with downregulation of IFN-γ expression and upregulation of PGES expression. ADSC, adipose-derived stem cell; IFN-γ, interferon gamma; PGES, prostaglandin E synthase.

Skin xenograft rejection correlated with IFN-γ expression levels, which is consistent with the results of previous studies (58, 60). IFN-γ can produce both immunostimulatory and immunosuppressive effects, depending on the spatiotemporal context (58, 61). However, little is known about the modulatory role of IFN-γ in skin xenotransplantation (62). In one study, injection of pig IFN-γ initiated the rejection of pig skin tissue transplanted into severely combined immunodeficient mice. Intradermal injections of recombinant pig IFN-γ increased the infiltration of neutrophils and macrophages into skin grafts (63). In a human-to-nude mouse xenotransplantation model, topical application of liposomal human recombinant IFN-γ induced the expression of intercellular adhesion molecule 1 (ICAM-1), a cell surface receptor that regulates the recruitment of leukocytes to inflammation sites (64, 65). Consistently, we observed that proinflammatory cytokine IFN-γ levels were decreased in the ADSC × 3 group, indicating improved survival of the xenografts.

In addition, the immunomodulatory effects of ADSCs in skin xenografts were associated with the PGES levels. High levels of PGE2 have been associated with the anti-inflammatory effects of MSCs, including suppression of proliferation and cytokine secretion by T lymphocytes (66, 67), induction of division arrest anergy of activated T cells (12) and induction of regulatory T cell proliferation (19, 68, 69). Moreover, PGE2 exerts immunosuppressive effects by inducing other soluble mediators such as IDO (20, 70). Further studies are needed to validate whether ADSC-mediated upregulation of PGE2 has a direct effect on the immune cell population within xenografts.

This study had some limitations. First, any effects of ADSCs in the presence

of immunosuppressants were not tested. Skin transplant patients may receive systemic or topical immunosuppressive agents that can affect the immunomodulatory capacity of ADSCs (47). Thus, in future studies, the combined effects of ADSCs and currently used immunosuppressants should be evaluated. Second, the survival and location of ADSCs were not evaluated. It would be useful to label ADSCs and evaluate how long they survive and whether they migrate to other tissues, such as regional lymph nodes (49, 69). Third, ADSCs are known to enhance graft survival through non-immune reactions such as angiogenic and antifibrotic responses. Therefore, the positive non-immune effects of ADSCs and the influence of immunomodulation on non-immune responses in skin xenografts should be evaluated.

The findings of this study suggest that multiple injections of ADSCs, compared to a single injection, have more potent immunosuppressive effects that lead to reduced cell-mediated rejection and prolonged graft survival in a human-to-rat xenotransplantation model. This dose-dependent effect of ADSCs was associated with the downregulation of IFN-γ and the upregulation of PGES.

References

1. Carrier AN, Verma A, Mohiuddin M, Pascual M, Muller YD, Longchamp A, et al. Xenotransplantation: A New Era. Front Immunol. 2022;13:900594.
2. Siemionow M, Nasir S. Immunologic responses in vascularized and nonvascularized skin allografts. J Reconstr Microsurg. 2008;24(7):497-505.
3. Simeonovic CJ, Townsend MJ, Karupiah G, Wilson JD, Zarb JC, Mann DA, et al. Analysis of the Th1/Th2 paradigm in transplantation: interferon-gamma deficiency converts Th1-type proislet allograft rejection to a Th2-type xenograft-like response. Cell Transplant. 1999;8(4):365-73.
4. Zhao Y, Xiong W, Yang T, Prall A, Baxter BT, Langnas AN. Xenogeneic skin graft rejection in M-CSF/macrophage deficient osteopetrotic mice. Xenotransplantation. 2003;10(3):232-9.
5. Yamamoto T, Iwase H, King TW, Hara H, Cooper DKC. Skin xenotransplantation: Historical review and clinical potential. Burns. 2018;44(7):1738-49.
6. Tomita Y, Uchida T, Zhang QW, Shimizu I, Iwai T, Yoshikawa M, et al. Human skin xenograft rejection in CD45 exon-6 knockout mice: the implication of involvement of a direct pathway. Surg Today. 2000;30(9):816-20.
7. Sykes M. Immunobiology of transplantation. FASEB J. 1996;10(7):721-30.
8. Gardner CR. The pharmacology of immunosuppressant drugs in skin transplant rejection in mice and other rodents. Gen Pharmacol. 1995;26(2):245-71.
9. Yanez R, Lamana ML, Garcia-Castro J, Colmenero I, Ramirez M, Bueren JA. Adipose tissue-derived mesenchymal stem cells have in vivo immunosuppressive properties applicable for the control of the graft-versus-host disease. Stem Cells. 2006;24(11):2582-91.
10. Castro-Manrreza ME, Montesinos JJ. Immunoregulation by mesenchymal stem cells: biological aspects and clinical applications. J Immunol Res. 2015;2015:394917.
11. Puissant B, Barreau C, Bourin P, Clavel C, Corre J, Bousquet C, et al. Immunomodulatory effect of human adipose tissue-derived adult stem cells: comparison with bone marrow mesenchymal stem cells. Br J Haematol.

2005;129(1):118-29.
12. Glennie S, Soeiro I, Dyson PJ, Lam EW, Dazzi F. Bone marrow mesenchymal stem cells induce division arrest anergy of activated T cells. Blood. 2005;105(7):2821-7.
13. Corcione A, Benvenuto F, Ferretti E, Giunti D, Cappiello V, Cazzanti F, et al. Human mesenchymal stem cells modulate B-cell functions. Blood. 2006;107(1):367-72.
14. Chen CC, Chen RF, Shao JS, Li YT, Wang YC, Brandacher G, et al. Adipose-derived stromal cells modulating composite allotransplant survival is correlated with B cell regulation in a rodent hind-limb allotransplantation model. Stem Cell Res Ther. 2020;11(1):478.
15. Zomer HD, Jeremias TDS, Ratner B, Trentin AG. Mesenchymal stromal cells from dermal and adipose tissues induce macrophage polarization to a pro-repair phenotype and improve skin wound healing. Cytotherapy. 2020;22(5):247-60.
16. Burchell JT, Strickland DH, Stumbles PA. The role of dendritic cells and regulatory T cells in the regulation of allergic asthma. Pharmacol Ther. 2010;125(1):1-10.
17. Leto Barone AA, Khalifian S, Lee WP, Brandacher G. Immunomodulatory effects of adipose-derived stem cells: fact or fiction? Biomed Res Int. 2013;2013:383685.
18. Cui L, Yin S, Liu W, Li N, Zhang W, Cao Y. Expanded adipose-derived stem cells suppress mixed lymphocyte reaction by secretion of prostaglandin E2. Tissue Eng. 2007;13(6):1185-95.
19. An JH, Song WJ, Li Q, Kim SM, Yang JI, Ryu MO, et al. Prostaglandin E2 secreted from feline adipose tissue-derived mesenchymal stem cells alleviate DSS-induced colitis by increasing regulatory T cells in mice. BMC Vet Res. 2018;14(1):354.
20. DelaRosa O, Lombardo E, Beraza A, Mancheno-Corvo P, Ramirez C, Menta R, et al. Requirement of IFN-gamma-mediated indoleamine 2,3-dioxygenase expression in the modulation of lymphocyte proliferation by human adipose-derived stem cells. Tissue Eng Part A. 2009;15(10):2795-806.
21. Ren G, Zhang L, Zhao X, Xu G, Zhang Y, Roberts AI, et al. Mesenchymal stem cell-mediated immunosuppression occurs via concerted action of chemokines

and nitric oxide. Cell Stem Cell. 2008;2(2):141-50.

22. Melief SM, Zwaginga JJ, Fibbe WE, Roelofs H. Adipose Tissue-Derived Multipotent Stromal Cells Have a Higher Immunomodulatory Capacity Than Their Bone Marrow-Derived Counterparts. Stem Cell Transl Med. 2013;2(6):455-63.

23. Hoogduijn MJ, Betjes MG, Baan CC. Mesenchymal stromal cells for organ transplantation: different sources and unique characteristics? Curr Opin Organ Transplant. 2014;19(1):41-6.

24. Lee SM, Lee SC, Kim SJ. Contribution of human adipose tissue-derived stem cells and the secretome to the skin allograft survival in mice. J Surg Res. 2014;188(1):280-9.

25. Larocca RA, Moraes-Vieira PM, Bassi EJ, Semedo P, de Almeida DC, da Silva MB, et al. Adipose tissue-derived mesenchymal stem cells increase skin allograft survival and inhibit Th-17 immune response. PLoS One. 2013;8(10):e76396.

26. Davis TA, Anam K, Lazdun Y, Gimble JM, Elster EA. Adipose-derived stromal cells promote allograft tolerance induction. Stem Cells Transl Med. 2014;3(12):1444-50.

27. Rosenberg AS, Singer A. Cellular basis of skin allograft rejection: an in vivo model of immune-mediated tissue destruction. Annu Rev Immunol. 1992;10:333-58.

28. Halloran PF, Einecke G, Sikosana MLN, Madill-Thomsen K. The Biology and Molecular Basis of Organ Transplant Rejection. Handb Exp Pharmacol. 2022;272:1-26.

29. Zhou J, He W, Luo G, Wu J. Fundamental immunology of skin transplantation and key strategies for tolerance induction. Arch Immunol Ther Exp (Warsz). 2013;61(5):397-405.

30. Wang J, Hao H, Huang H, Chen D, Han Y, Han W. The Effect of Adipose-Derived Stem Cells on Full-Thickness Skin Grafts. Biomed Res Int. 2016;2016:1464725.

31. Zografou A, Tsigris C, Papadopoulos O, Kavantzas N, Patsouris E, Donta I, et al. Improvement of skin-graft survival after autologous transplantation of adipose-derived stem cells in rats. J Plast Reconstr Aesthet Surg. 2011;64(12):1647-56.

32. Vidor SB, Terraciano PB, Valente FS, Rolim VM, Kuhl CP, Ayres LS, et al. Adipose-derived stem cells improve full-thickness skin grafts in a rat model. Res Vet Sci. 2018;118:336-44.

33. Kroemer A, Xiao X, Degauque N, Edtinger K, Wei H, Demirci G, et al. The innate NK cells, allograft rejection, and a key role for IL-15. J Immunol. 2008;180(12):7818-26.

34. Abumaree M, Al Jumah M, Pace RA, Kalionis B. Immunosuppressive properties of mesenchymal stem cells. Stem Cell Rev Rep. 2012;8(2):375-92.

35. Fiori A, Uhlig S, Kluter H, Bieback K. Human Adipose Tissue-Derived Mesenchymal Stromal Cells Inhibit CD4+ T Cell Proliferation and Induce Regulatory T Cells as Well as CD127 Expression on CD4+CD25+ T Cells. Cells. 2021;10(1).

36. Haddad R, Saldanha-Araujo F. Mechanisms of T-cell immunosuppression by mesenchymal stromal cells: what do we know so far? Biomed Res Int. 2014;2014:216806.

37. Morikawa S, Mabuchi Y, Kubota Y, Nagai Y, Niibe K, Hiratsu E, et al. Prospective identification, isolation, and systemic transplantation of multipotent mesenchymal stem cells in murine bone marrow. J Exp Med. 2009;206(11):2483-96.

38. Kim H, Hyun MR, Kim SW. The Effect of Adipose-Derived Stem Cells on Wound Healing: Comparison of Methods of Application. Stem Cells Int. 2019;2019:2745640.

39. Hong KY, Kim IK, Park SO, Jin US, Chang H. Systemic Administration of Adipose-Derived Stromal Cells Concurrent with Fat Grafting. Plast Reconstr Surg. 2019;143(5):973e-82e.

40. Eggenhofer E, Luk F, Dahlke MH, Hoogduijn MJ. The life and fate of mesenchymal stem cells. Front Immunol. 2014;5:148.

41. Kuo YR, Chen CC, Goto S, Lee IT, Huang CW, Tsai CC, et al. Modulation of immune response and T-cell regulation by donor adipose-derived stem cells in a rodent hind-limb allotransplant model. Plast Reconstr Surg. 2011;128(6):661e-72e.

42. Duijvestein M, Vos AC, Roelofs H, Wildenberg ME, Wendrich BB, Verspaget HW, et al. Autologous bone marrow-derived mesenchymal stromal cell treatment for refractory luminal Crohn's disease: results of a phase I study. Gut. 2010;59(12):1662-9.

43. Gao F, Chiu SM, Motan DA, Zhang Z, Chen L, Ji HL, et al. Mesenchymal stem cells and immunomodulation: current status and future prospects. Cell Death Dis. 2016;7(1):e2062.
44. Keating A. Mesenchymal stromal cells: new directions. Cell Stem Cell. 2012;10(6):709-16.
45. Yang CH, Wang GJ, Ma FF, Yu BQ, Chen FC, Yang J, et al. Repeated injections of human umbilical cord blood-derived mesenchymal stem cells significantly promotes functional recovery in rabbits with spinal cord injury of two noncontinuous segments. Stem Cell Research & Therapy. 2018;9.
46. Mahmoud EE, Adachi N, Mawas AS, Deie M, Ochi M. Multiple intra-articular injections of allogeneic bone marrow-derived stem cells potentially improve knee lesions resulting from surgically induced osteoarthritis: an animal study. Bone Joint J. 2019;101-B(7):824-31.
47. Plock JA, Schnider JT, Schweizer R, Zhang W, Tsuji W, Waldner M, et al. The Influence of Timing and Frequency of Adipose-Derived Mesenchymal Stem Cell Therapy on Immunomodulation Outcomes After Vascularized Composite Allotransplantation. Transplantation. 2017;101(1):e1-e11.
48. Zhou X, Ning K, Ling B, Chen X, Cheng H, Lu B, et al. Multiple Injections of Autologous Adipose-Derived Stem Cells Accelerate the Burn Wound Healing Process and Promote Blood Vessel Regeneration in a Rat Model. Stem Cells Dev. 2019;28(21):1463-72.
49. Jeon S, Ha JH, Kim I, Bae J, Kim SW. The Immunomodulatory Effect of Adipose-Derived Stem Cells in Xenograft Transplantation Model. Transplant Proc. 2022.
50. Manning DD, Reed ND, Shaffer CF. Maintenance of skin xenografts of widely divergent phylogenetic origin of congenitally athymic (nude) mice. J Exp Med. 1973;138(2):488-94.
51. Cendales LC, Kanitakis J, Schneeberger S, Burns C, Ruiz P, Landin L, et al. The Banff 2007 working classification of skin-containing composite tissue allograft pathology. Am J Transplant. 2008;8(7):1396-400.
52. Luo Y, Yi X, Liang T, Jiang S, He R, Hu Y, et al. Autograft microskin combined with adipose-derived stem cell enhances wound healing in a full-thickness skin defect mouse model. Stem Cell Res Ther. 2019;10(1):279.

53. Wolbank S, Peterbauer A, Fahrner M, Hennerbichler S, van Griensven M, Stadler G, et al. Dose-dependent immunomodulatory effect of human stem cells from amniotic membrane: a comparison with human mesenchymal stem cells from adipose tissue. Tissue Eng. 2007;13(6):1173-83.

54. Hu JL, Kim BJ, Yu NH, Kwon ST. Impact of Injection Frequency of Adipose-Derived Stem Cells on Allogeneic Skin Graft Survival Outcomes in Mice. Cell Transplant. 2021;30:9636897211041966.

55. Lorenzi W, Goncalves FDC, Schneider N, Silva EF, Visioli F, Paz AH, et al. Repeated systemic administration of adipose tissue-derived mesenchymal stem cells prevents tracheal obliteration in a murine model of bronchiolitis obliterans. Biotechnol Lett. 2017;39(8):1269-77.

56. Benichou G, Yamada Y, Yun SH, Lin C, Fray M, Tocco G. Immune recognition and rejection of allogeneic skin grafts. Immunotherapy. 2011;3(6):757-70.

57. Fairchild RL. The Yin and Yang of IFN-gamma in allograft rejection. Am J Transplant. 2003;3(8):913-4.

58. Hidalgo LG, Halloran PF. Role of IFN-gamma in allograft rejection. Crit Rev Immunol. 2002;22(4):317-49.

59. Moss MI, Pauli M, Moreau JM, Cohen JN, Rosenblum MD, Lowe MM. Xenograft Skin Model to Manipulate Human Immune Responses In Vivo. J Vis Exp. 2022(184).

60. Famulski KS, Sis B, Billesberger L, Halloran PF. Interferon-gamma and donor MHC class I control alternative macrophage activation and activin expression in rejecting kidney allografts: a shift in the Th1-Th2 paradigm. Am J Transplant. 2008;8(3):547-56.

61. Zhang YJ, Wang YC, Wu GF, Zhang W, Wang XJ, Cai WX, et al. Prolonged skin grafts survival time by IFN-gamma in allogeneic skin transplantation model during acute rejection through IFN-gamma/STAT3/IDO pathway in epidermal layer. Biochem Bioph Res Co. 2018;496(2):436-42.

62. Wang H, DeVries ME, Deng S, Khandaker MH, Pickering JG, Chow LH, et al. The axis of interleukin 12 and gamma interferon regulates acute vascular xenogeneic rejection. Nat Med. 2000;6(5):549-55.

63. Sultan P, Murray AG, McNiff JM, Lorber MI, Askenase PW, Bothwell AL,

et al. Pig but not human interferon-gamma initiates human cell-mediated rejection of pig tissue in vivo. Proc Natl Acad Sci U S A. 1997;94(16):8767-72.

64. Bui TM, Wiesolek HL, Sumagin R. ICAM-1: A master regulator of cellular responses in inflammation, injury resolution, and tumorigenesis. J Leukoc Biol. 2020;108(3):787-99.

65. Short SM, Paasch BD, Turner JH, Weiner N, Daugherty AL, Mrsny RJ. Percutaneous absorption of biologically-active interferon-gamma in a human skin graft-nude mouse model. Pharm Res. 1996;13(7):1020-7.

66. Zafranskaya M, Nizheharodava D, Yurkevich M, Ivanchik G, Demidchik Y, Kozhukh H, et al. PGE2 contributes to in vitro MSC-mediated inhibition of non-specific and antigen-specific T cell proliferation in MS patients. Scand J Immunol. 2013;78(5):455-62.

67. Yanez R, Oviedo A, Aldea M, Bueren JA, Lamana ML. Prostaglandin E2 plays a key role in the immunosuppressive properties of adipose and bone marrow tissue-derived mesenchymal stromal cells. Exp Cell Res. 2010;316(19):3109-23.

68. Ghannam S, Pene J, Moquet-Torcy G, Jorgensen C, Yssel H. Mesenchymal stem cells inhibit human Th17 cell differentiation and function and induce a T regulatory cell phenotype. J Immunol. 2010;185(1):302-12.

69. Bassi EJ, Moraes-Vieira PM, Moreira-Sa CS, Almeida DC, Vieira LM, Cunha CS, et al. Immune regulatory properties of allogeneic adipose-derived mesenchymal stem cells in the treatment of experimental autoimmune diabetes. Diabetes. 2012;61(10):2534-45.

70. Ma S, Xie N, Li W, Yuan B, Shi Y, Wang Y. Immunobiology of mesenchymal stem cells. Cell Death Differ. 2014;21(2):216-25.

Abstract in Korean

배경: 지방유래 줄기세포 (Adipose-derived stem cell, ADSC)는 동종 피부 이식 모델에서 면역 조절 효과를 보이는 것으로 알려져 있다. 이 연구는 인간 피부 이종 이식 모델에서 ADSC의 면역조절 효과를 검증하고, 그 작용 기전을 분석하는 것을 목표로 한다.

방법: C57BL/6 마우스 등에 전층 인간 피부를 이식한 후 ADSC를 정맥주사와 국소 피하 주사로 투여하였으며, 각각의 투여 방법이 이식편 생존에 미치는 영향을 비교 분석하였다. 보다 상세한 면역 기전을 파악하기 위해 Sprague-Dawley rat (SD 랫드) 등에 인간 피부 이종 이식 실험을 시행하였다. ADSC (1×10^6 cells/ml)를 수술 직후 단일로 투여하거나 수술 후 0일, 3일, 그리고 5일에 각각 3회 투여하여, 투여 빈도가 이식편 생존 및 면역 조절 효과에 미치는 영향을 비교 분석하였다. 이식 후 7일, 10일, 그리고 14일에 피부 이식편, 액와 림프절, 혈청을 수집하여 면역 세포의 침투 정도, proinflammatory cytokine인 interferon-γ (IFN-γ), 그리고 ADSC가 분비하는 anti-inflammatory factor인 prostaglandin E2 synthase (PGES)의 발현을 분석하였다.

결과: 인간-마우스 이종 피부 이식 모델에서는 ADSC를 국소 피하 주사로 투여하는 것이 정맥주사보다 이식편 생존을 더욱 향상시켰다. 인간-랫드 이종 피부 이식 모델에서는 ADSC를 3회 투여하는 것이 수술 직후 단일 투여보다 세포 매개 이종 이식 거부 반응을 4일 정도 지연시켰다. ADSC를 3회 투여하였을 때 이식 거부 반응이 감소하였으며, 이는 이식편의 표피 기저층에서 세포 분열이 증가하고, 미세혈관 생성 밀도가 더욱 증가한 결과로 나타났다. 이식편 내의 CD3, CD4, CD8, $CD68^+$ 면역 세포(T 세포, 대식세포) 침투는 감소하였고, 피부 이식편과 주변 액와 림프절에서는 IFN-γ 발현이 줄어들고, PGES 발현이 증가한 것을 확인했다.

결론: 이 연구를 통해 인간 피부 이종 이식 모델에서 ADSC가 세포 매개 이식 거부 반응을 저해하며, 이로 인해 이식편 생존이 증가하는 것을 확인하였다. 이 결과는 피부 이식편과 주변 림프절에서 IFN-γ 발현의 감소와 PGES 발현의 증가와 관련이 있음을 시사한다.